

Supplementary Information for

WNT/RYK signaling functions as an anti-inflammatory modulator in the lung mesenchyme

Hyun-Taek Kim, Paolo Panza, Khrievono Kikhi, Yuko Nakamichi, Ann Atzberger, Stefan Guenther, Clemens Ruppert, Andreas Guenther, and Didier Y.R. Stainier

Correspondence and requests for materials should be addressed to H.-T.K. (email: hyun-taek.kim@sch.ac.kr) or D.Y.R.S. (email: didier.stainier@mpi-bn.mpg.de).

This PDF file includes:

Supplementary text

Supplementary methods

SI References

Figures S1 to S11

Tables S1 to S2

Legends for Datasets S1

Methods

Mouse strains

We described the *Ryk*^{SL} and *Ryk* floxed mouse lines previously (1). *Dermo1-Cre* (2) was purchased from The Jackson Laboratory. The following mouse lines were kindly provided for our study: *Rosa26-CreER*^{T2} (3) by Dr. Thomas Braun; *Tek-CreER*^{T2} (4) by Dr. Stefan Offermanns; *Gli1-CreER*^{T2} (5) by Dr. Saverio Bellusci; *Lyz2-Cre* (6) by Dr. Christian Stockmann. Tamoxifen (Sigma) was dissolved in corn oil (Sigma) at 50 mg/ml and injected intraperitoneally at the indicated developmental stages and frequencies. Pan-caspase inhibitor (Z-VAD-FMK, Santa Cruz Biotechnology) and Caspase-3 inhibitor (Z-DEVD-FMK, TOCRIS) were dissolved in DMSO and injected intraperitoneally in lactating mothers at the indicated developmental stages and frequencies at 10 mg/kg. Evans blue dye (Sigma) was dissolved in 0.9 % NaCl and intracardially injected at P3, as previously described (7). All animal care and experimental procedures in this study were approved by the local animal ethics committee at the Regierungspräsidium Darmstadt, Hessen, Germany. To genotype all transgenic mice, the following PCR protocol was used: 95 °C for 3 min, 35 cycles of 95 °C for 30 sec, 57 °C for 30 sec and 72 °C for 30 sec. The following primers were used: *Cre* forward 5'-GAC CAG GTT CGT TCA CTC ATG G-3' and *Cre* reverse 5'-AGG CTA AGT GCC TTC TCT ACA C-3', *Cre-ER* forward 5'-GCT AAG GAT GAC TCT GGT CAG-3' and *Cre-ER* reverse 5'-CAG CAT CCA ACA AGG CAC TG-3', *Ryk* floxed forward 5'-TCA TTA ACC AAA ACA TCT CGC-3' and *Ryk* floxed reverse 5'-ACC CTG CCT CCA AAA ACA AA-3'.

Plasmids

Total RNA and cDNA were obtained from E18.5 lungs using TRIzol (Life Technologies) and Superscript III reverse transcriptase (Life Technologies), respectively, according to manufacturer's instructions. To synthesize RNA probes for in situ hybridization, cDNA was PCR-amplified using total cDNA from E18.5 lungs as a template. PCR fragments were cloned into pGEM T-easy vector (Promega). The following primers were used: *Bcl3* (NCBI, Acc. No. NM_033601) forward 5'-CGT GGA CCT GGA GGT TCG CAA T-3' and *Bcl3* reverse 5'-GGC AGG TGT AGA TGT TGT GGG AA-3'; *Casp4* (NCBI, Acc. No. NM_007609) forward 5'-GAA GAC TTA GGC TAC GAT GTG GT-3' and *Casp4* reverse 5'-CTC AGT TGC CAG GAA AGA GGT AG-3'; *Ccl2* (NCBI, Acc. No. NM_011333) forward 5'-ACC ATG CAG GTC CCT GTC ATG CTT-3' and *Ccl2* reverse 5'-GAG TCA CAC TAG TTC ACT GTC ACA-3'; *Fas* (NCBI, Acc. No. NM_007987) forward 5'-TTC TAC TGC GAT TCT CCT GGC TG-3' and *Fas* reverse 5'-GTT TTC ACT CCA GAC ATT GTC C-3'.

Flow cytometry analysis

To sort the different lung cell types including epithelial cells, endothelial cells, hematopoietic cells, and mesenchymal cells, P2 *Dermo1-Ryk*^{WT} and *Dermo1-Ryk*^{CKO} lungs were digested with Dispase II (Sigma) in DMEM (Dulbecco's Modified Eagle Media). Homogenized lungs were passed through a 70 µm nylon mesh to obtain a single-cell suspension. Cells were incubated with Fc Block for 30 mins at 4 °C, washed, and stained for 1 hour at 4 °C with an

antibody mixture containing EpCAM-APC (BioLegend, 1:200), CD45-PE (BioLegend, 1:200), and CD31-FITC (BioLegend, 1:100). Cell suspension was filtered through a 35 μ m nylon mesh (Falcon®, 352235) just before sorting. Cells were sorted with a BD FACSAria III cell sorter (BD Biosciences) with a 100 μ m nozzle. Dead cells were excluded using DAPI (Sigma). For immune cell phenotyping, P3 *Dermo1-Ryk^{WT}* and *Dermo1-Ryk^{ckO}* lungs were digested with Dispase II in DMEM. Homogenized lungs were passed through a 70 μ m nylon mesh to obtain a single-cell suspension. Cells were stained using a mixture of fluorochrome-conjugated antibodies. The following antibodies were used: CD11b-PE-Cy5 (BioLegend, 1:200), CD11c-PE (eBiosciences, 1:200), CD45-APC-Cy7 (BioLegend, 1:200), F4/80-FITC (BioLegend, 1:100), Ly6g-BV421 (BD Biosciences, 1:200), and SiglecF-APC (BioLegend, 1:200). DAPI was used to exclude dead cells. Cells were analysed on a BD LSRFortessa equipped with 5 lasers. Single stained controls and 'Fluorescence minus one (FMO)' controls were used to set the compensation settings and define the gating region for the target population. Post-acquisition analysis was performed using the FACS Diva software (BD Biosciences).

Histology and TUNEL

For paraffin sections, whole lungs were fixed in 4% paraformaldehyde, embedded in paraffin and sectioned at a thickness of 5 μ m. For cryosections, fixed tissues were embedded in OCT and 10 μ m thick coronal sections were collected. Hematoxylin and eosin (H&E) was performed according to standard protocols. For apoptotic cell detection, frozen tissue sections were stained using an *In situ* Apoptosis Detection Kit (MK500, Takara) according to manufacturer's instructions.

***In situ* hybridization and immunohistochemistry**

In situ hybridization using digoxigenin-labelled RNA probes was performed as previously described (8). Immunohistochemistry was performed according to a standard protocol. The following antibodies and lectin were used for immunostaining at the indicated dilution: α -smooth muscle actin-Cy3 (Sigma, 1:1000), CASP4 (Sigma, 1:500), CCL2 (Novus Biologicals, 1:200), CD3 (BioLegend, 1:500), CD19 (BioLegend, 1:500), CD11C (eBioscience, 1:500), CD45 (BioRad, 1:500). Cleaved CASP3 (Cell Signaling, 1:200), E-Cadherin (Santa Cruz Biotechnology, 1:500), ELASTIN (Abcam, 1:1000), F4/80 (BioRad, 1:500), Isolectin-B4-FITC (Sigma, 1:500), Ki-67 (Invitrogen, 1:500), MAC2 (Invitrogen, 1:500), MYH10 (Sigma, 1:500), PCNA (Dako, 1:200), PECAM-1 (BD Biosciences, 1:500)

Cell culture, siRNA knockdowns, and Western Blot analysis

The NIH3T3 mouse embryonic fibroblasts (9) were maintained at 37 °C in a 5% CO₂ incubator in DMEM, supplemented with 10% FBS, 50 g/ml streptomycin, 50 U/ml penicillin. siRNAs for *EGFP* (EHUEGFP, Sigma) and *Ryk* (EMU085001, Sigma) were transfected using RNAiMAX transfection reagent (133778, Life Technologies) according to manufacturer's instructions. WNT-3A (400-022, ReliaTech, Germany) and WNT-5A (400-023, ReliaTech, Germany) recombinant proteins were used at 500 ng/ml. Western blotting was performed according to standard protocols. Primary antibodies were incubated overnight at 4 °C in 3% skim milk. The following antibodies and dilutions were used for immunoblotting:

CTNNB1/ β -catenin (BD Biosciences, 1:1000), Phospho-CTNNB1/ β -catenin (Ser33/37/Thr41) (Cell Signaling, 1:1000), CCL2 (Santa Cruz Biotechnology, 1:1000), Cleaved CASP3 (Cell Signaling, 1:1000), CASPASE4 (Sigma, 1:2000), GAPDH (Santa Cruz Biotechnology, 1:1000), I κ B α (Cell Signaling, 1:1000), Phospho-I κ B α (S32/36) (Cell Signaling, 1:1000), I κ K α β (Cell Signalling, 1:1000), Phospho-I κ K α β (S176/180) (Cell Signaling, 1:1000), NF- κ B/P65 (Cell Signaling, 1:1000), Phospho-NF- κ B/P65 (Ser536) (Cell Signaling, 1:1000). Uncropped images related to western blots are included in [SI Appendix, Fig. S11](#).

RT-qPCR

Total RNA and cDNA were obtained from sorted lung cells, cultured cells, and postnatal lungs using TRIzol reagent (Life Technologies) and Superscript III reverse transcriptase (Life Technologies), respectively, according to the manufacturer's instructions. For quantitative reverse transcription PCR, the CFX Connect Real-Time system (Bio-Rad) and DyNAmo colorFlash SYBR green qPCR kit (ThermoFisher Scientific) were used. The primer sequences for qPCR are shown in [SI Appendix, Table S1](#). The Ct values are shown in [SI Appendix, Table S2](#).

Transcriptomic analysis

For RNAseq, total RNA was isolated from P0 lungs (left lobes) of three *Dermol-Ryk^{WT}* and three *Dermol-Ryk^{KO}* mice using Trizol reagent (Life Technologies) combined with on-column DNase digestion (TURBO DNase, Ambion) to avoid contamination by genomic DNA. RNA sequencing was performed as previously described (8). To examine the biological significance of the DEGs, we carried out a Gene Ontology (GO) enrichment analysis using the online tool Database for Annotation, Visualization and Integrated Discovery (DAVID) Bioinformatics Resource v6.8 (<https://david.ncifcrf.gov/home.jsp>).

Statistical analysis

Data are presented as mean \pm s.e.m of at least three biological replicates. Two-tailed Student's t-tests were used to assess significance. A P-value of < 0.05 was considered significant.

References in Materials and Methods

1. H. T. Kim et al., WNT/RYK signaling restricts goblet cell differentiation during lung development and repair. *Proc Natl Acad Sci U S A* 116, 25697-25706 (2019).
2. D. Susic, J. A. Richardson, K. Yu, D. M. Ornitz, E. N. Olson, Twist regulates cytokine gene expression through a negative feedback loop that represses NF-kappaB activity. *Cell* 112, 169-180 (2003).
3. A. Ventura et al., Restoration of p53 function leads to tumour regression in vivo. *Nature* 445, 661-665 (2007).
4. H. Korhonen et al., Anaphylactic shock depends on endothelial Gq/G11. *J Exp Med* 206, 411-420 (2009).

5. S. Ahn, A. L. Joyner, Dynamic changes in the response of cells to positive hedgehog signaling during mouse limb patterning. *Cell* 118, 505-516 (2004).
6. B. E. Clausen, C. Burkhardt, W. Reith, R. Renkawitz, I. Forster, Conditional gene targeting in macrophages and granulocytes using LysMcre mice. *Transgenic Res* 8, 265-277 (1999).
7. T. Walchli et al., Quantitative assessment of angiogenesis, perfused blood vessels and endothelial tip cells in the postnatal mouse brain. *Nat Protoc* 10, 53-74 (2015).
8. H. T. Kim et al., Myh10 deficiency leads to defective extracellular matrix remodeling and pulmonary disease. *Nat Commun* 9, 4600 (2018).
9. G. J. Todaro, H. Green, Quantitative studies of the growth of mouse embryo cells in culture and their development into established lines. *J Cell Biol* 17, 299-313 (1963).

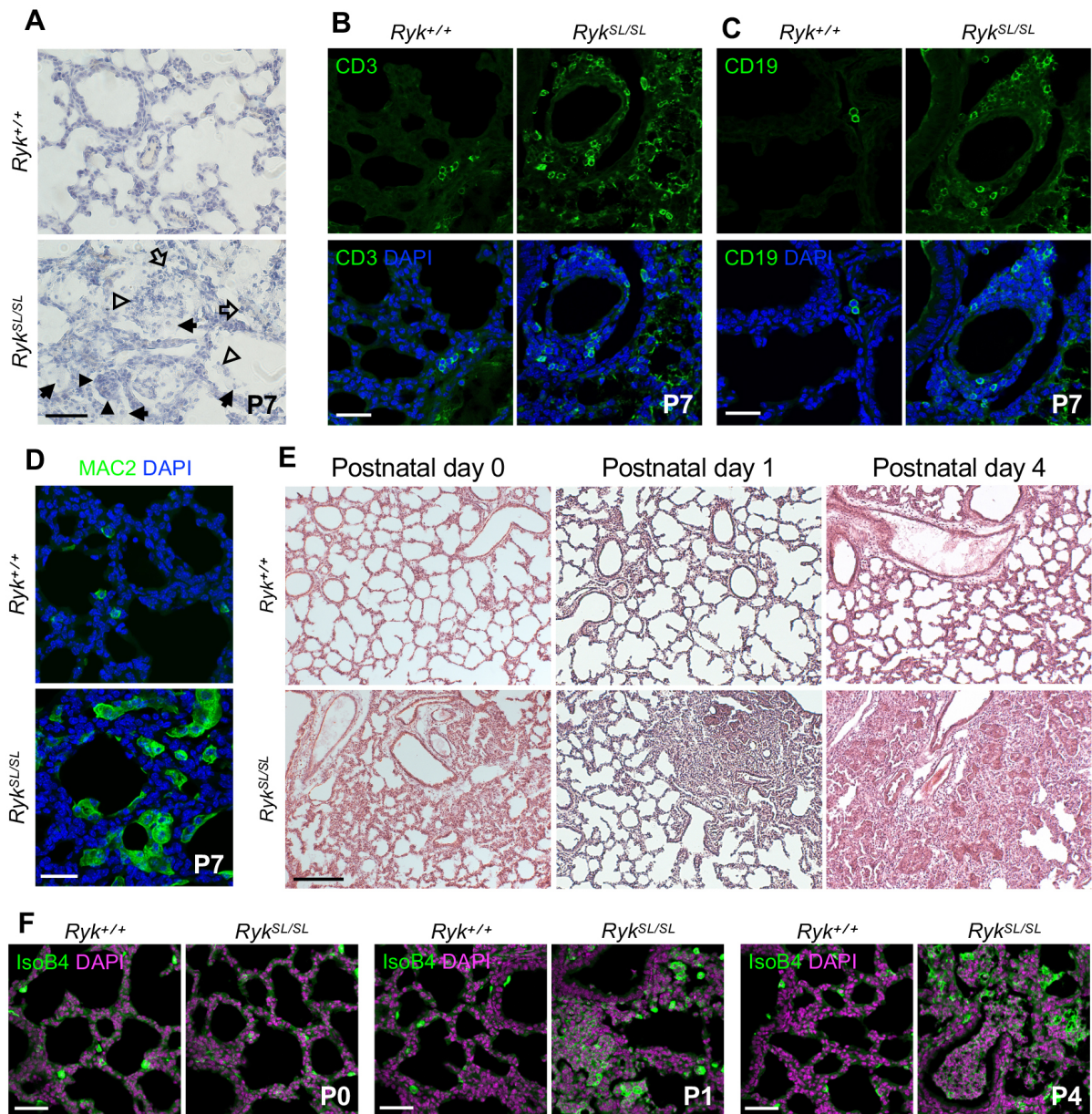


Fig. S1. *Ryk^{SL/SL}* mice exhibit lung inflammation at postnatal stages. (A) Hematoxylin staining of P7 *Ryk^{+/+}* (n=10) and *Ryk^{SL/SL}* (n=12) lung sections. Arrows, macrophages; arrowheads, lymphocytes; open arrows, neutrophils; open arrowheads, monocytes. (B) Immunostaining for CD3 (to mark lymphocytes (T-cells)) in P7 *Ryk^{+/+}* (n=10) and *Ryk^{SL/SL}* (n=12) lung sections. (C) Immunostaining for CD19 (to mark lymphocytes (B-cells)) in P7 *Ryk^{+/+}* (n=10) and *Ryk^{SL/SL}* (n=12) lung sections. (D) Immunostaining for MAC2 (alveolar and interstitial macrophages) in P7 *Ryk^{+/+}* (n=10) and *Ryk^{SL/SL}* (n=12) lung sections. (E) H&E staining of *Ryk^{+/+}* (n=6) and *Ryk^{SL/SL}* (n=6) lung sections at P0, P1, and P4. (F) Isolectin B4 staining (to mark immune cells) of *Ryk^{+/+}* (n=6) and *Ryk^{SL/SL}* (n=6) lung sections at P0, P1, and P4. Scale bars: 100 μ m (E), 50 μ m (F), and 30 μ m (B-D).

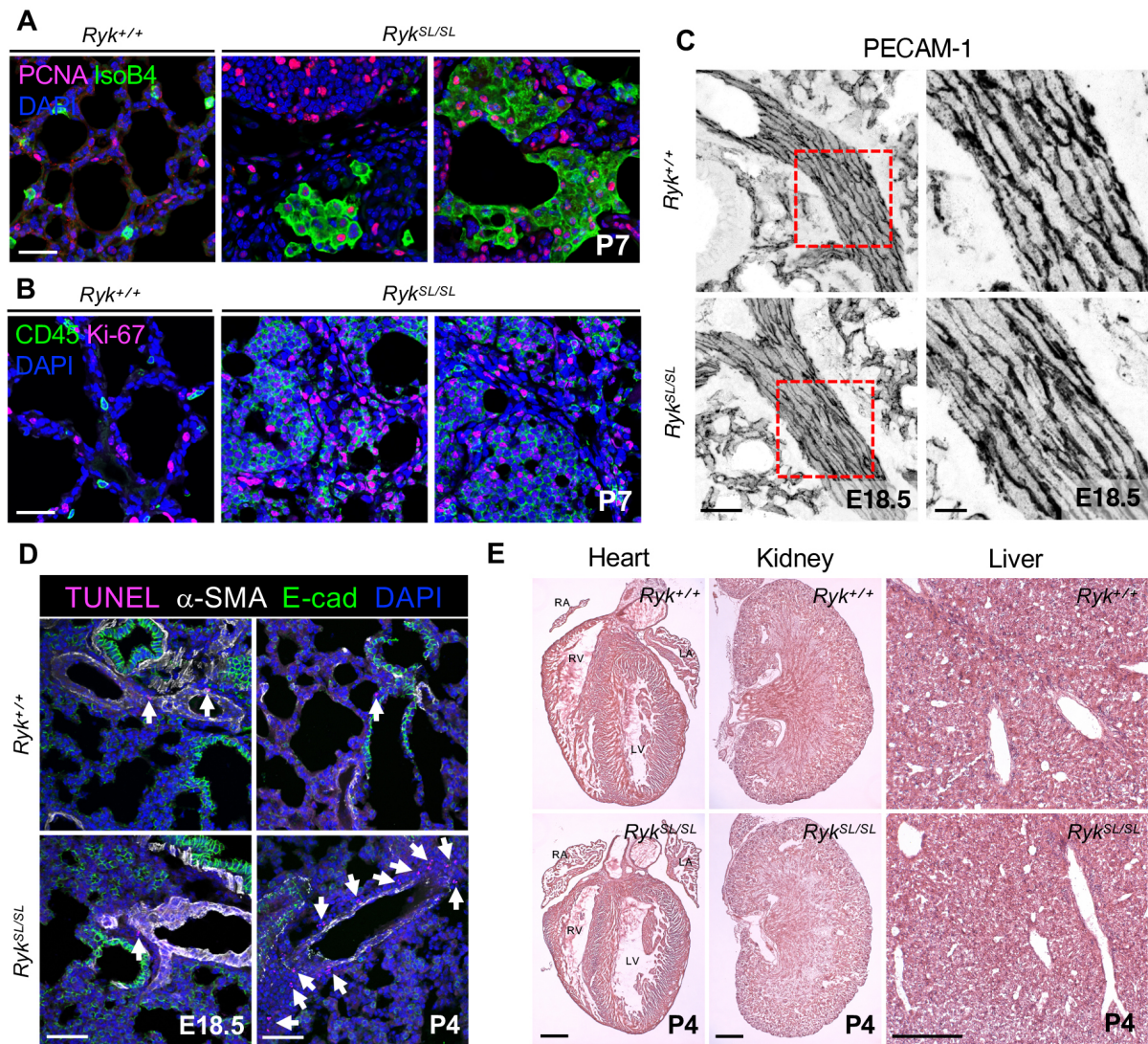


Fig. S2. *Ryk^{SL/SL}* mice exhibit lung mesenchymal cell death and vessel integrity defects at postnatal stages. (A) IsoB4 staining (to mark immune cells) and PCNA immunostaining (to mark proliferating cells) in P7 *Ryk^{+/+}* (n=10) and *Ryk^{SL/SL}* (n=12) lung sections. (B) Immunostaining for CD45 (hematopoietic cells) and for Ki-67 (to mark proliferating cells) in P7 *Ryk^{+/+}* (n=10) and *Ryk^{SL/SL}* (n=12) lung sections. (C) Immunostaining for PECAM-1 (to mark endothelial cells) in E18.5 *Ryk^{+/+}* (n=10) and *Ryk^{SL/SL}* (n=12) lung sections. High-magnification image of the areas in the dashed boxes is shown on the right. (D) TUNEL staining and immunostaining for α -SMA (to mark myofibroblasts and smooth muscle cells) and E-cadherin (to mark epithelial cells) in *Ryk^{+/+}* (n=6) and *Ryk^{SL/SL}* (n=6) lung sections at E18.5 and P4. Arrows point to TUNEL-positive cells. (E) H&E staining of P4 *Ryk^{+/+}* (n=6) and *Ryk^{SL/SL}* (n=12) heart, kidney and liver sections. Abbreviations: LA, left atrium; LV, left ventricle; RA, right atrium; RV, right ventricle. Scale bars: 500 μ m (E), 50 μ m (D), 30 μ m (A, B, C (left)), and 10 μ m (C (right)).

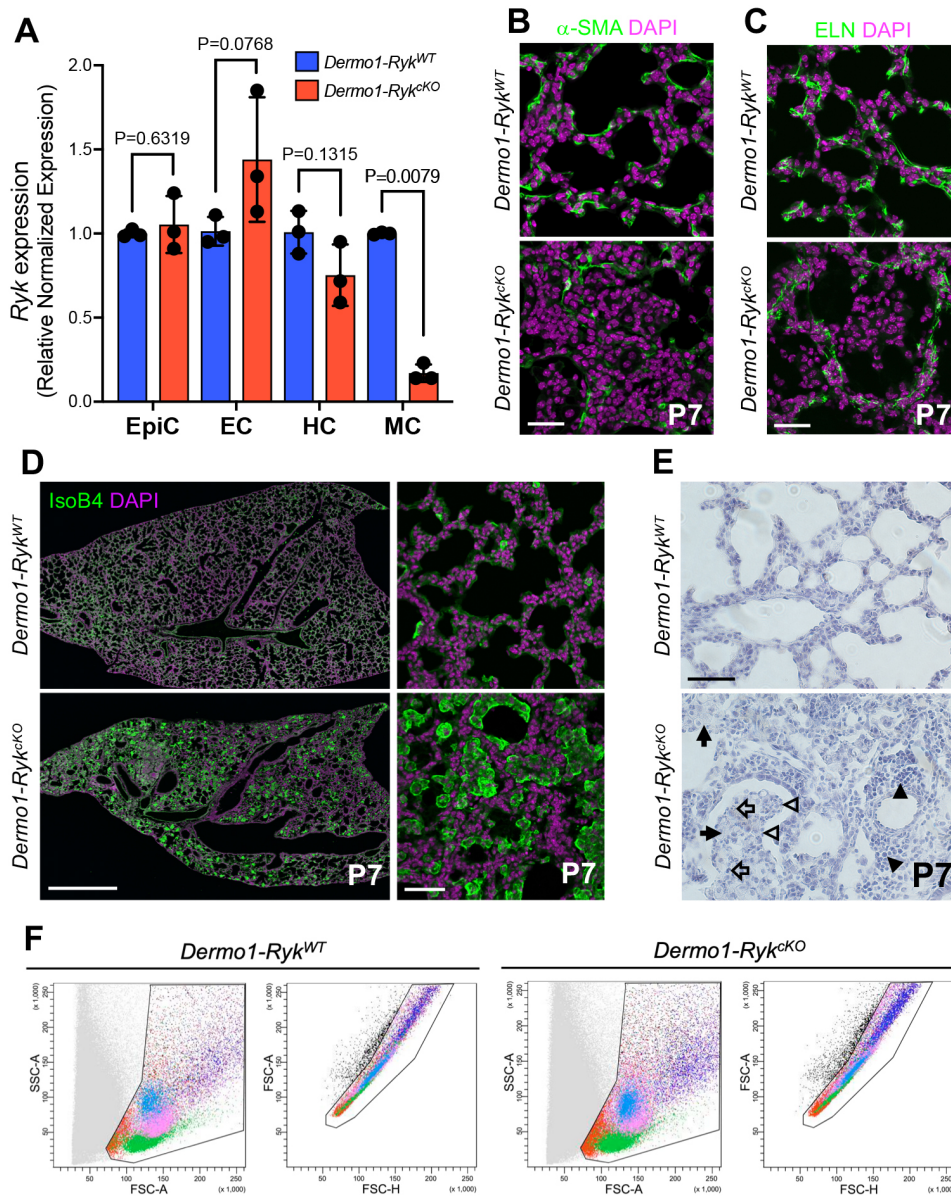


Fig. S3. *Dermo1-Ryk^{CKO}* mice exhibit lung inflammation and defective alveolar formation at postnatal stages. (A) qPCR analysis of *Ryk* mRNA levels in epithelial cells (EpiC), endothelial cells (EC), hematopoietic cells (HC), and mesenchymal cells (MC) of *Dermo1-Ryk^{WT}* (n=3) and *Dermo1-Ryk^{CKO}* (n=3) lungs at P3. (B) Immunostaining for α -SMA (to mark myofibroblasts) in P7 *Dermo1-Ryk^{WT}* (n=10) and *Dermo1-Ryk^{CKO}* (n=9) lung sections. (C) Immunostaining for ELN (to mark secondary septa) in P7 *Dermo1-Ryk^{WT}* (n=10) and *Dermo1-Ryk^{CKO}* (n=9) lung sections. (D) IsoB4 staining (to mark immune cells) in P7 *Dermo1-Ryk^{WT}* (n=10) and *Dermo1-Ryk^{CKO}* (n=9) lung sections. (E) Hematoxylin staining of P7 *Dermo1-Ryk^{WT}* (n=10) and *Dermo1-Ryk^{CKO}* (n=9) lung sections. Arrows, macrophages; arrowheads, lymphocytes; open arrows, neutrophils; open arrowheads, monocytes. (F) Immunophenotyping of immune cell populations in the lung of P3 *Dermo1-Ryk^{WT}* and *Dermo1-Ryk^{CKO}* mice. Error bars are means \pm s.e.m., two-tailed Student's *t* test. Ct values are listed in Table S2. Scale bars: 1 mm (D (left)), 50 μ m (D (right) and E), and 30 μ m (B and C).

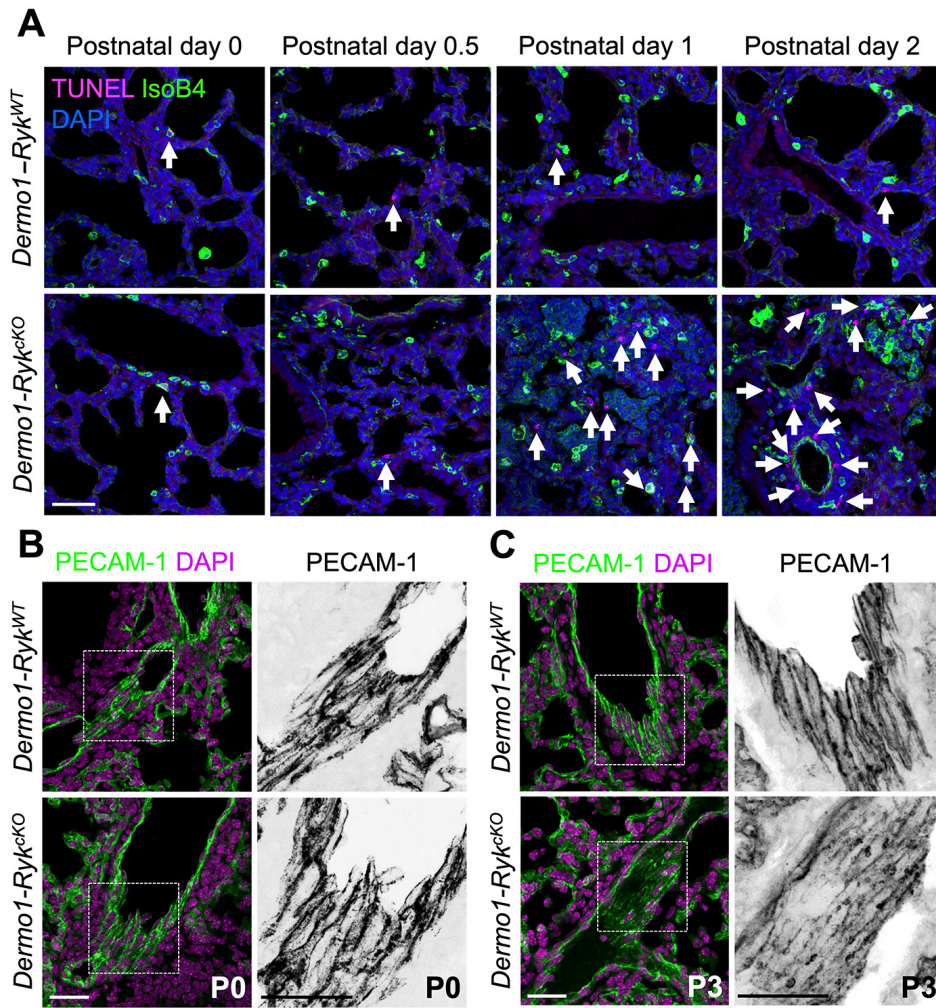


Fig. S4. *Dermo1-Ryk^{CKO}* mice exhibit lung mesenchymal cell death and vessel integrity defects at postnatal stages. (A) TUNEL staining and IsoB4 staining (to mark immune cells) in *Dermo1-Ryk^{WT}* (n=3) and *Dermo1-Ryk^{CKO}* (n=3) lung sections at P0, P0.5, P1, and P2. Arrows point to TUNEL-positive cells. (B) Immunostaining for PECAM-1 in P0 *Dermo1-Ryk^{WT}* (n=6) and *Dermo1-Ryk^{CKO}* (n=6) lung sections. High-magnification image of the areas in the dashed boxes is shown on the right. (C) Immunostaining for PECAM-1 in P3 *Dermo1-Ryk^{WT}* (n=6) and *Dermo1-Ryk^{CKO}* (n=6) lung sections. High-magnification image of the areas in the dashed boxes is shown on the right. Scale bars: 50 μm (A) and 30 μm (B and C).

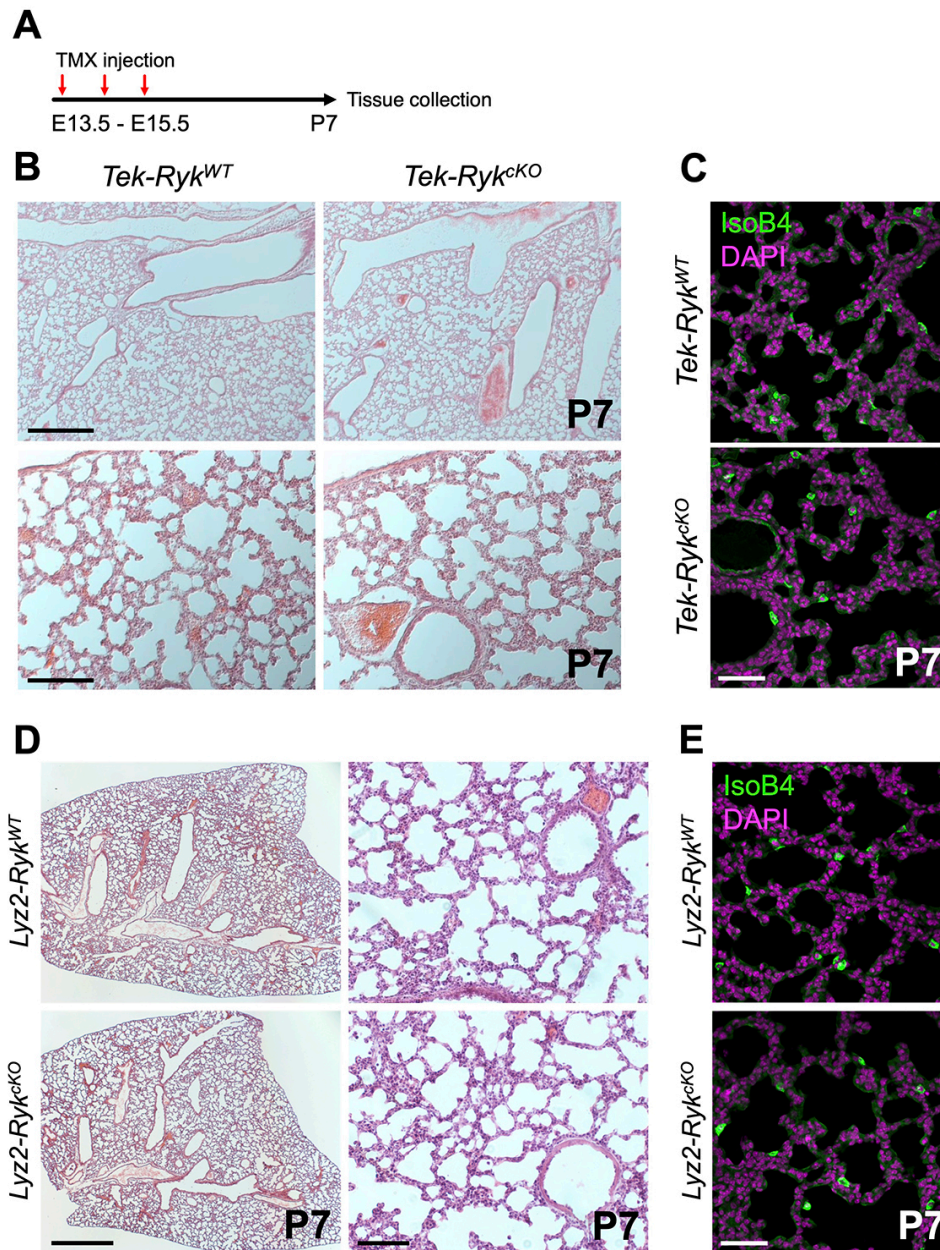


Fig. S5. Endothelial and myeloid cell-specific *Ryk* deletion does not cause any obvious lung phenotypes. (A) Diagram indicating the time points of tamoxifen injections and tissue collection in early postnatal *Tek-Ryk^{KO}* mice. (B) H&E staining of P7 *Tek-Ryk^{WT}* (n=6) and *Tek-Ryk^{KO}* (n=6) lung sections. (C) IsoB4 staining (to mark immune cells) in P7 *Tek-Ryk^{WT}* (n=6) and *Tek-Ryk^{KO}* (n=6) lung sections. (D) H&E staining of P7 *Lyz2-Ryk^{WT}* (n=6) and *Lyz2-Ryk^{KO}* (n=6) lung sections. (E) IsoB4 staining (to mark immune cells) in P7 *Lyz2-Ryk^{WT}* (n=6) and *Lyz2-Ryk^{KO}* (n=6) lung sections. Scale bars: 1 mm (D), 400 μ m (B (top)), 100 μ m (D (right)), and 50 μ m (B (bottom), C, E).

A

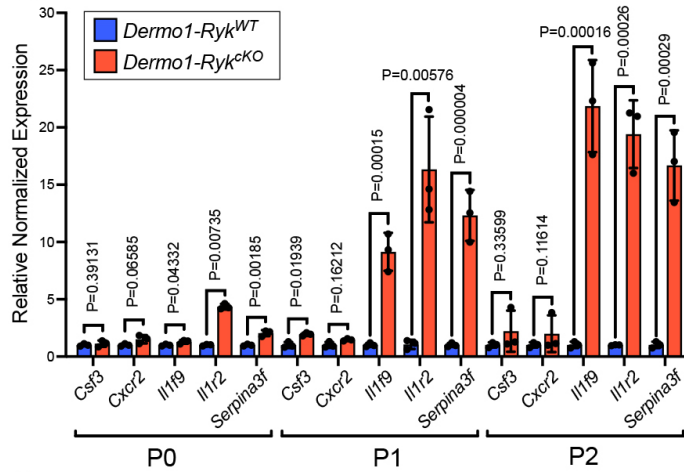
Up-regulated genes

Terms	Biological function	No. of genes	P-Value
GO:0002376	Immune system process	11	2.4E-4
GO:0045766	Positive regulation of angiogenesis	6	1.3E-3
GO:0034097	Response to cytokine	5	2.1E-3
GO:0002244	Hematopoietic progenitor cell differentiation	5	4.1E-3
GO:0006915	Apoptotic process	11	4.7E-3
GO:0030593	Neutrophil chemotaxis	4	1.1E-2

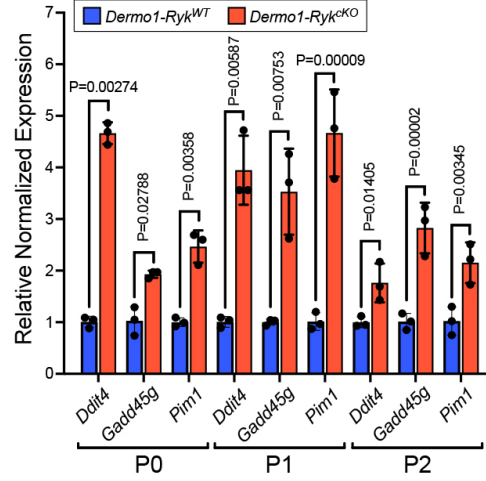
Down-regulated genes

Terms	Biological function	No. of genes	P-Value
GO:0045165	Cell fate commitment	4	4.3E-3
GO:0007275	Multicellular organism development	11	1.8E-2
GO:0060487	Lung epithelial cell differentiation	2	5.3E-2
GO:0003073	Regulation of systemic arterial blood pressure	2	5.7E-2
GO:0055117	Regulation of cardiac muscle contraction	2	8.3E-2

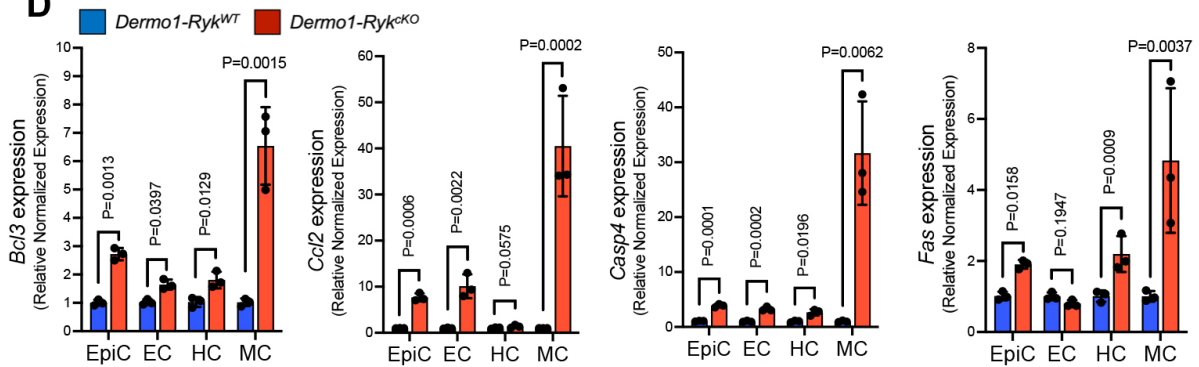
B



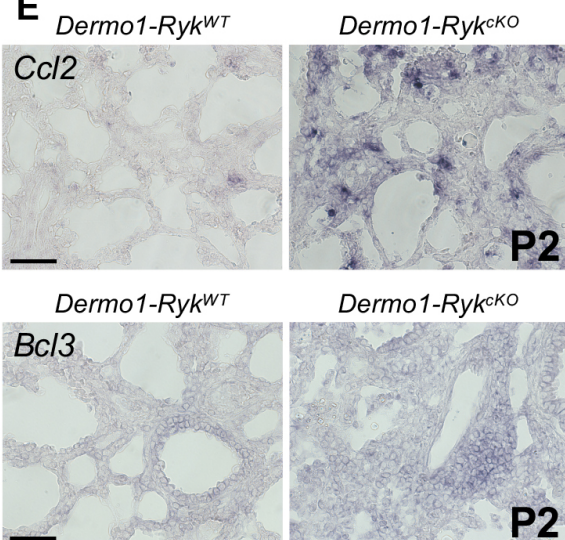
C



D



E



F

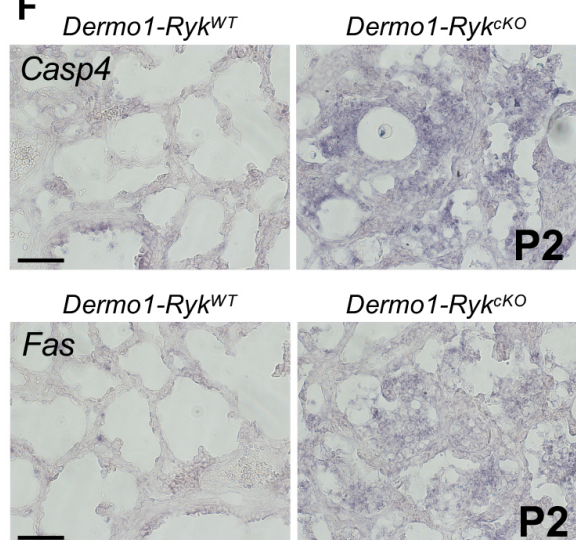


Fig. S6. Loss of *Ryk* function in the mesenchyme leads to upregulation of inflammatory and pro-apoptotic genes in the lungs. (A) Gene ontology classification of differentially expressed genes between P0 *Dermo1-Ryk^{WT}* (n=3) and *Dermo1-Ryk^{CKO}* (n=3) lungs from RNAseq analysis. (B) qPCR analysis of *Csf3*, *Cxcr2*, *Il1f9*, *Il1r2*, and *Serpina3f* mRNA levels in *Dermo1-Ryk^{WT}* (n=3) and *Dermo1-Ryk^{CKO}* (n=3) lungs at P0, P1, and P2. (C) qPCR analysis of *Ddit4*, *Gadd45g*, and *Pim1* mRNA levels in *Dermo1-Ryk^{WT}* (n=3) and *Dermo1-Ryk^{CKO}* (n=3) lungs at P0, P1, and P2. (D) qPCR analysis of *Bcl3*, *Ccl2*, *Casp4*, and *Fas* mRNA levels in epithelial cells (EpiC), endothelial cells (EC), hematopoietic cells (HC), and mesenchymal cells (MC) of *Dermo1-Ryk^{WT}* (n=3) and *Dermo1-Ryk^{CKO}* (n=3) lungs at P2. (E) Expression of *Ccl2* and *Bcl3* mRNA in P2 *Dermo1-Ryk^{WT}* (n=3) and *Dermo1-Ryk^{CKO}* (n=3) lung sections by *in situ* hybridization. (F) Expression of *Casp4* and *Fas* mRNA in P2 *Dermo1-Ryk^{WT}* (n=3) and *Dermo1-Ryk^{CKO}* (n=3) lung sections by *in situ* hybridization. Error bars are means \pm s.e.m, two-tailed Student's *t* test. Ct values are listed in [Table S2](#). Scale bars: 50 μ m (E and F).

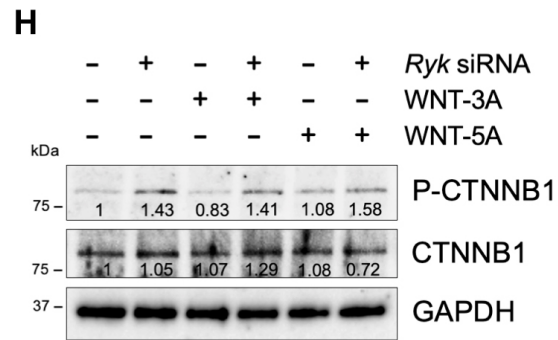
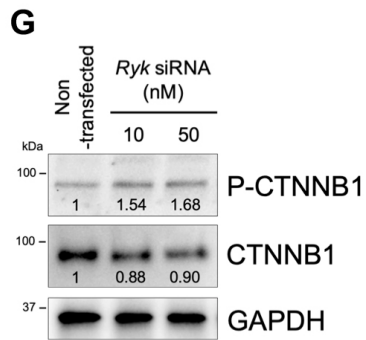
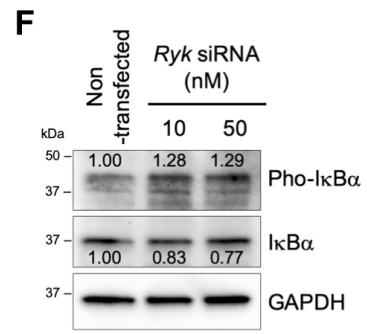
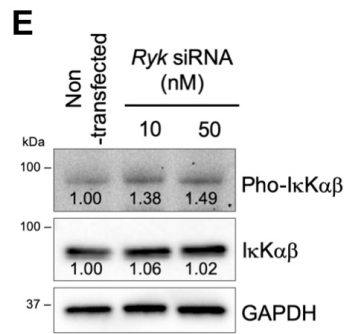
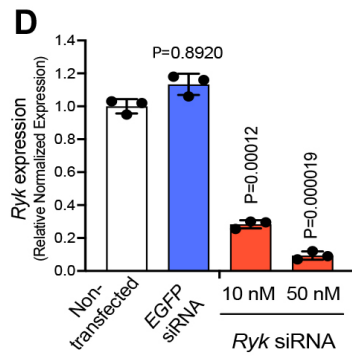
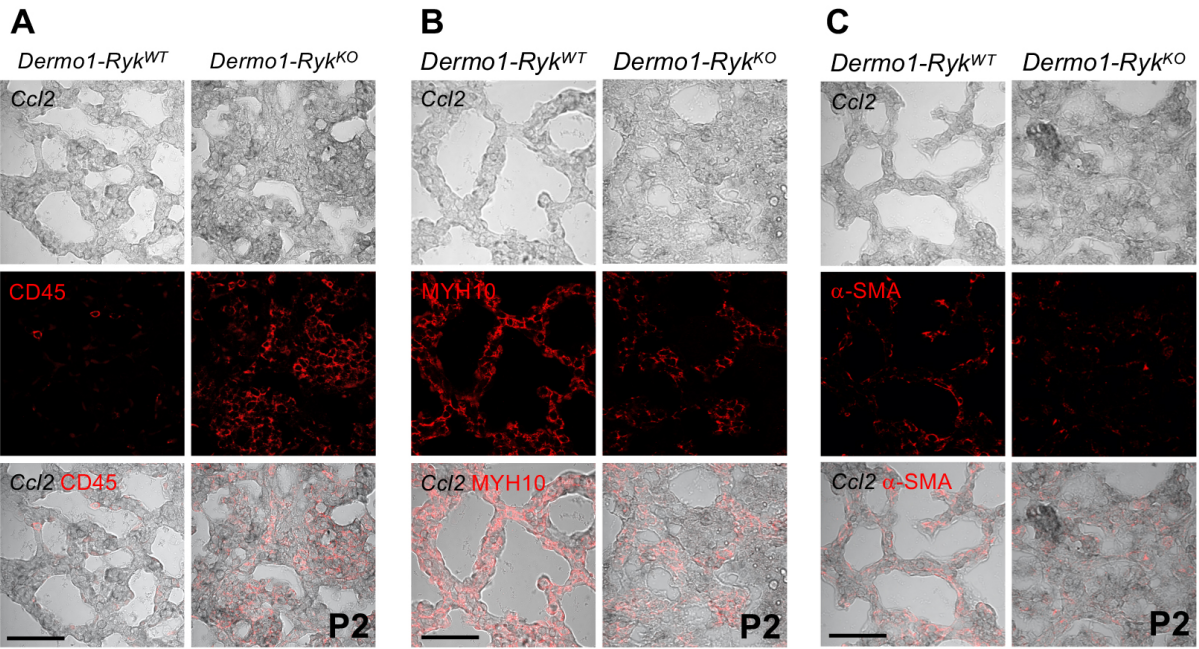


Fig. S7. RYK participates in WNT/ β -catenin signaling in fibroblasts. (A) Double staining for *Ccl2* (mRNA) and CD45 (hematopoietic cells) in P2 *Dermo1-Ryk^{WT}* (n=6) and *Dermo1-Ryk^{cKO}* (n=6) lung sections. (B) Double staining for *Ccl2* (mRNA) and MYH10 (to mark mesenchymal cells) in P2 *Dermo1-Ryk^{WT}* (n=6) and *Dermo1-Ryk^{cKO}* (n=6) lung sections. (C) Double staining for *Ccl2* (mRNA) and α -SMA (to mark myofibroblasts) in P2 *Dermo1-Ryk^{WT}* (n=6) and *Dermo1-Ryk^{cKO}* (n=6) lung sections. (D) qPCR analysis of *Ryk* mRNA levels in non-transfected, *EGFP* siRNA, and *Ryk* siRNA (10 nM or 50 nM) transfected NIH3T3 fibroblasts. (E) Representative western blot (from three individual sets of cell lysates) for I κ K $\alpha\beta$ and Phospho-I κ K $\alpha\beta$ in NIH3T3 fibroblasts after *Ryk* knockdown. Values represent densitometric ratios after normalization to GAPDH, except for Phospho-I κ K $\alpha\beta$ which was normalized to GAPDH and total I κ K $\alpha\beta$. (F) Representative western blot (from three individual sets of cell lysates) for I κ B α and Phospho-I κ B α in NIH3T3 fibroblasts after *Ryk* knockdown. Values represent densitometric ratios after normalization to GAPDH, except for Phospho-I κ B α , which was normalized to GAPDH and total I κ B α . (G) Representative western blot (from three individual sets of cell lysates) for CTNNB1 and Phospho-CTNNB1 in NIH3T3 fibroblasts after *Ryk* knockdown. Values represent densitometric ratios after normalization to GAPDH, except Phospho-CTNNB1, which was normalized to GAPDH and total CTNNB1. (H) Representative western blot (from three individual sets of cell lysates) for CTNNB1 and Phospho-CTNNB1 upon stimulation with WNT-3A or WNT-5A and/or co-transfection of *Ryk* siRNA in NIH3T3 fibroblasts. Values represent densitometric ratios after normalization to GAPDH, except for Phospho-CTNNB1, which was normalized to GAPDH and total CTNNB1. Error bars are means \pm s.e.m., two-tailed Student's *t* test. Ct values are listed in [Table S2](#). Scale bars: 50 μ m (A, B, C).

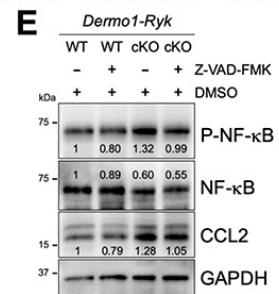
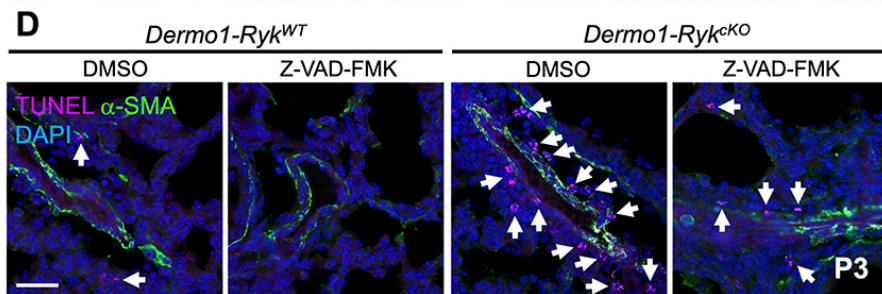
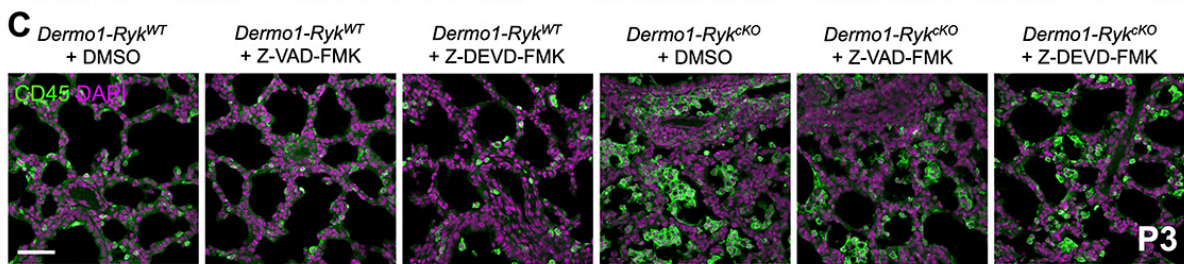
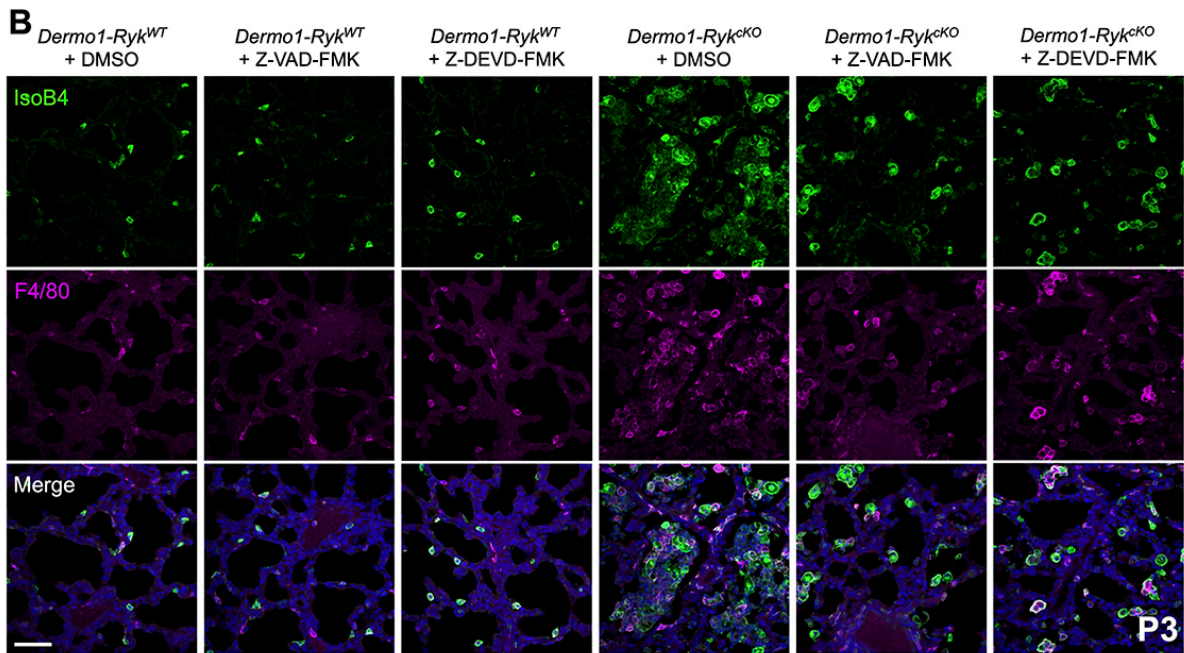
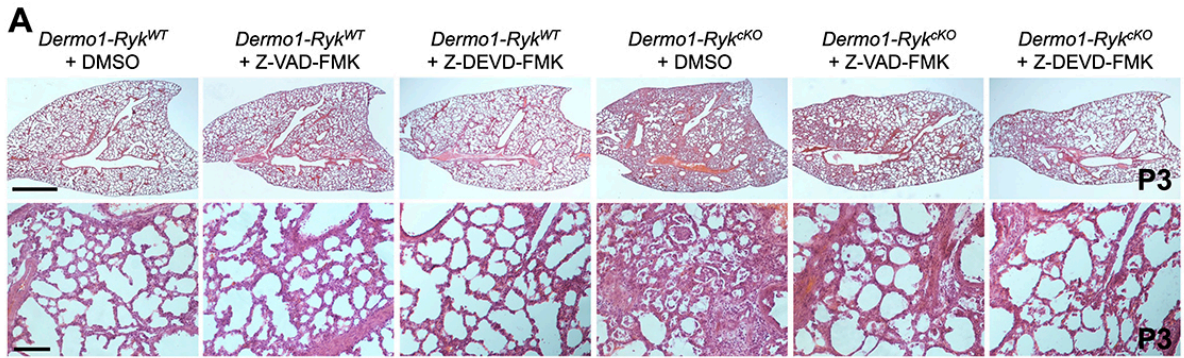


Fig. S8. Blocking apoptosis partially rescues the lung phenotypes of *Dermo1-Ryk^{CKO}* mice. (A) H&E staining of lung sections from DMSO, Z-VAD-FMK, or Z-DEVD-FMK injected P3 *Dermo1-Ryk^{WT}* (n=6) and *Dermo1-Ryk^{CKO}* (n=6) animals. (B) IsoB4 staining (to mark immune cells) and F4/80 immunostaining (alveolar and interstitial macrophages) in DMSO, Z-VAD-FMK, and Z-DEVD-FMK treated P3 *Dermo1-Ryk^{WT}* (n=6) and *Dermo1-Ryk^{CKO}* (n=6) lung sections. (C) Immunostaining for CD45 (hematopoietic cells) in DMSO, Z-VAD-FMK, or Z-DEVD-FMK treated P3 *Dermo1-Ryk^{WT}* (n=6) and *Dermo1-Ryk^{CKO}* (n=6) lung sections. (D) TUNEL staining and α -SMA immunostaining (to mark myofibroblasts and smooth muscle cells) in DMSO or Z-VAD-FMK treated P3 *Dermo1-Ryk^{WT}* (n=6) and *Dermo1-Ryk^{CKO}* (n=6) lung sections. Arrows point to TUNEL-positive cells. (E) Representative western blot (from three individual sets of lung lysates) for NF- κ B, Phospho-NF- κ B, and CCL2 in DMSO or Z-VAD-FMK treated P3 *Dermo1-Ryk^{WT}* and *Dermo1-Ryk^{CKO}* lungs. Values represent densitometric ratios after normalization to GAPDH, except for Phospho-NF- κ B, which was normalized to GAPDH and total NF- κ B. Scale bars: 1 mm (A (top)), 100 μ m (A (bottom)), and 50 μ m (B-D).

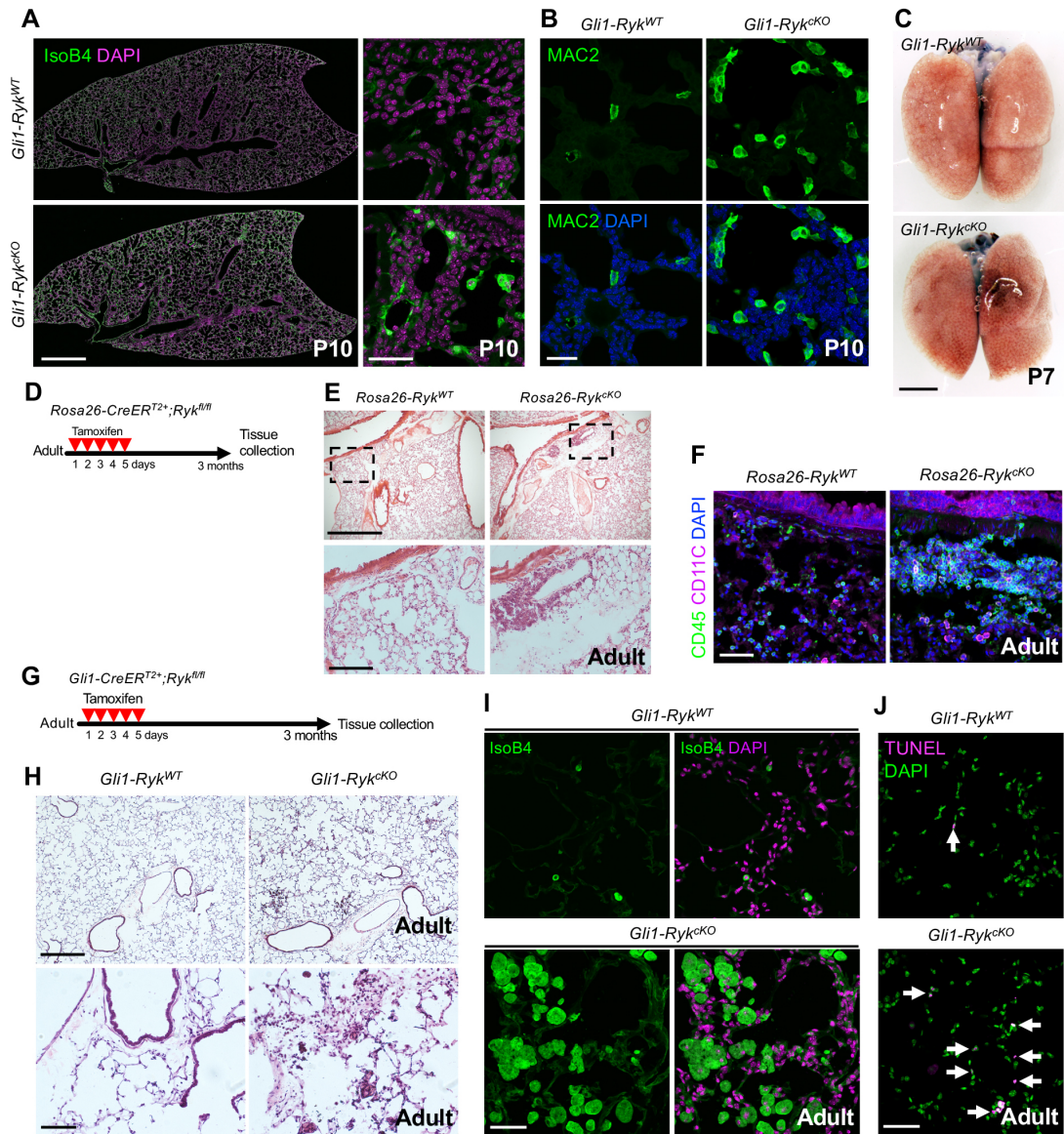


Fig. S9. Loss of *Ryk* leads to inflammatory cell accumulation during lung maturation and homeostasis. (A) IsoB4 staining (to mark immune cells) of P10 *Gli1-Ryk*^{WT} (n=6) and *Gli1-Ryk*^{cKO} (n=6) lung sections. (B) Immunostaining for MAC2 (alveolar and interstitial macrophages) in P10 *Gli1-Ryk*^{WT} (n=6) and *Gli1-Ryk*^{cKO} (n=6) lung sections. (C) Representative images of P7 *Gli1-Ryk*^{WT} (n=6) and *Gli1-Ryk*^{cKO} (n=3) lungs injected with Evans Blue dye. (D) Diagram indicating the time points of tamoxifen injections and tissue collection in adult *Rosa26-Ryk*^{cKO} mice. (E) H&E staining of adult *Rosa26-Ryk*^{WT} (n=5) and *ROSA26-Ryk*^{cKO} (n=5) lung sections. High-magnification image of the areas in the dashed boxes is shown on the bottom. (F) Immunostaining for CD45 (hematopoietic cells) and CD11C (monocytes and granulocytes) in adult *Rosa26-Ryk*^{WT} (n=5) and *Rosa26-Ryk*^{cKO} (n=5) lung sections. (G) Diagram indicating the time points of tamoxifen injections and tissue collection in adult *Gli1-Ryk*^{cKO} mice. (H) H&E staining of adult *Gli1-Ryk*^{WT} (n=5) and *Gli1-Ryk*^{cKO} (n=5) lung sections. (I) IsoB4 staining (to mark immune cells) of adult *Gli1-Ryk*^{WT} (n=5) and *Gli1-Ryk*^{cKO} (n=5) lung sections. (J) TUNEL staining of adult *Gli1-Ryk*^{WT} (n=5) and *Gli1-Ryk*^{cKO} (n=5) lung sections. Arrows point to TUNEL-positive cells. Scale bars: 1mm (A (left)), 500 µm (E and H (Top)), 200 µm (C), 100 µm (E and H (Bottom)), 50 µm (F, I, J), and 30 µm (A (right)).

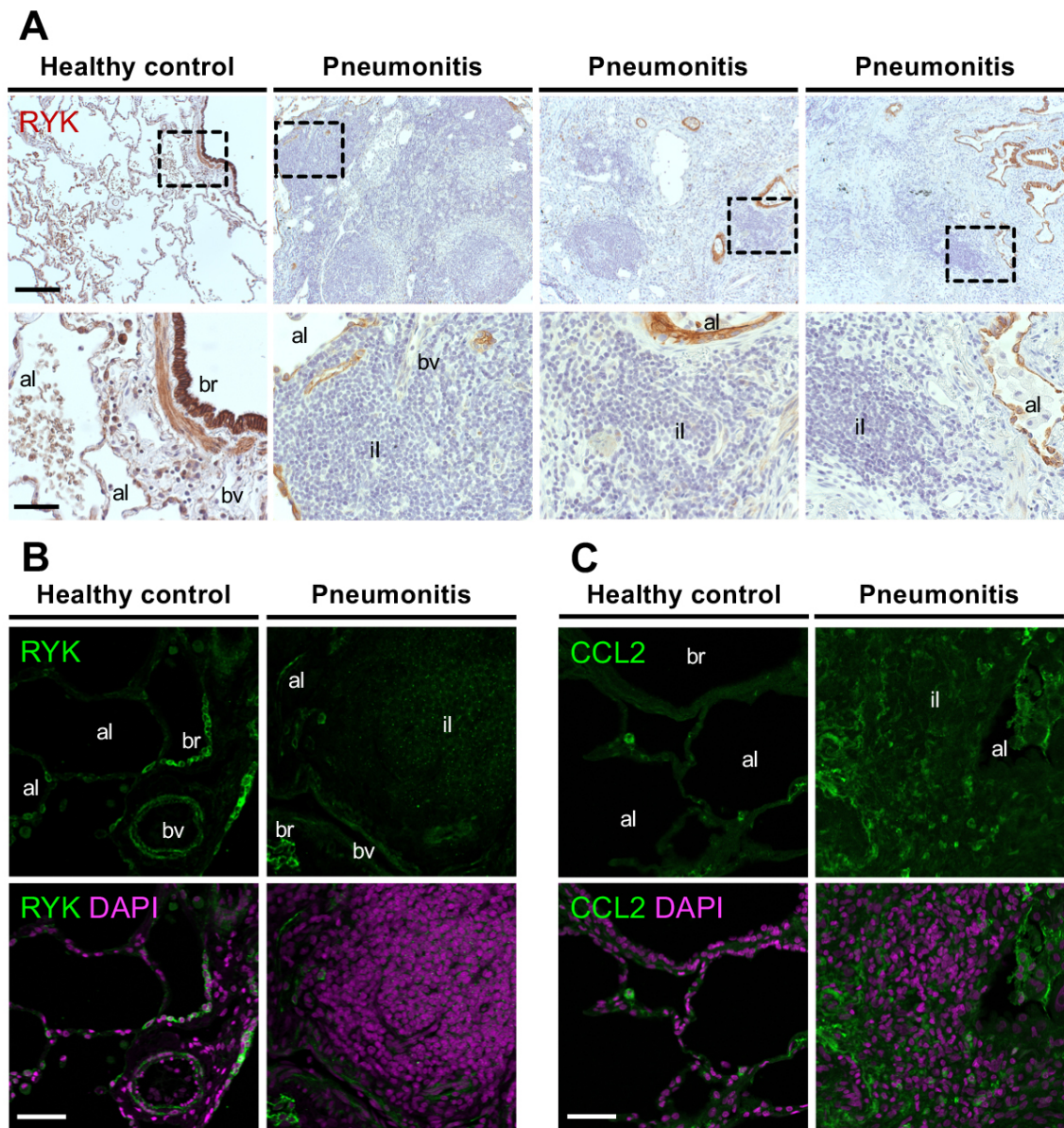


Fig. S10. Reduced RYK expression and increased CCL2 expression in stromal cells of pneumonitis lungs. (A) Immunostaining for RYK in the lungs of healthy controls (n=5) and pneumonitis patients (n=10). High-magnification image of the areas in the dashed boxes is shown on the bottom. (B) Fluorescent immunostaining for RYK in the lungs of healthy controls (n=5) and pneumonitis patients (n=10). (C) Fluorescent immunostaining for CCL2 in the lungs of healthy controls (n=5) and pneumonitis patients (n=10). Abbreviations: al, alveoli; br, bronchiole; bv, blood vessel; il, inflammatory lesion. Scale bars: 200 μ m (A (Top)) and 50 μ m (A (Bottom), B, C).

Fig. S11. Uncropped images related to western blotting data

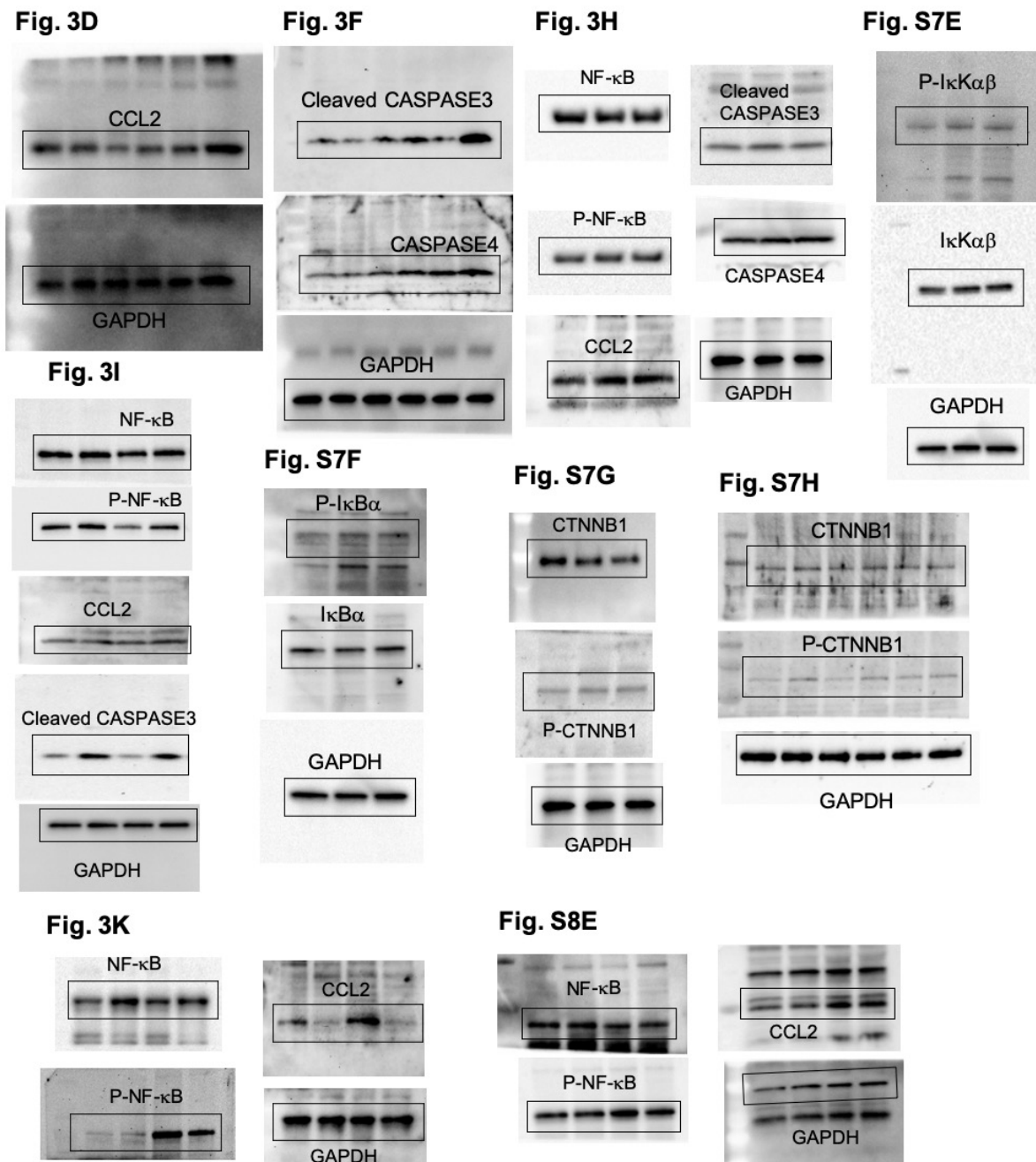


Table S1. Sequence of primers used for RT-qPCR analysis

Gene name	Forward primer (5'-3')	Reverse primer (5'-3')
<i>Bcl3</i>	AGCAGTCGTCTCAGCTCCAATG	AGGCAGGTGTAGATGTTGTGGG
<i>Casp4</i>	GTGGTGAAAGAGGAGCTTACAGC	GCACCAGGAATGTGCTGTCTGA
<i>Ccl2</i>	CTTCTGGGCCTGCTGTTCA	CCAGCCTACTCATTGGGATCA
<i>Csf3</i>	ATCCCGAAGGCTTCCCTGAGTG	AGGAGACCTTGGTAGAGGCAGA
<i>Cxcr2</i>	CTCTATTCTGCCAGATGCTGTCC	ACAAGGCTCAGCAGAGTCACCA
<i>Ddit4</i>	ACTGCGAGTCCCTGGACAGCA	TTGGCACACAGGTGCTCATCCT
<i>Fas</i>	ATGCACACTCTGCGATGAAG	CAGTGTTCCACAGCCAGGAGA
<i>Gadd45g</i>	TCTACGAGTCCGCCAAAGTCCT	CTCACAGCAGAACGCCTGAATC
<i>Gapdh</i>	TGTGTCCGTCGTGGATCTGA	CCTGCTTACCACCTTCTTGAT
<i>Il1f9</i>	TTGACTTGACCAGCAGGTGTG	GGGTACTTGCATGGGAGGATAG
<i>Il1r2</i>	CCATGAAGGCCAGCAATACCACATCAC	CGGGATTGTCAGTCTTGACCCAGAG
<i>Pim1</i>	CGCGACATCAAGGACGAGAACA	CGAATCCACTCTGGAGGACTGT
<i>Ryk</i>	GACCTCATCAGTCACTACGC	GTACAAGAAAGCTCGACCCG
<i>Serpina3f</i>	ACTACAGCCTGGAGCACATCCT	ACATCCAGCACAGCCTTGTGGA

Table S2. mRNA expression levels were analyzed by RT-qPCR

Fig. 3B

Sample Name	Gene Name	Ct mean
P0 <i>Dermo1-Ryk^{WT}</i>	<i>Bcl3</i>	29.49
P0 <i>Dermo1-Ryk^{CKO}</i>	<i>Bcl3</i>	28.79
P1 <i>Dermo1-Ryk^{WT}</i>	<i>Bcl3</i>	31.67
P1 <i>Dermo1-Ryk^{CKO}</i>	<i>Bcl3</i>	28.29
P2 <i>Dermo1-Ryk^{WT}</i>	<i>Bcl3</i>	31.46
P2 <i>Dermo1-Ryk^{CKO}</i>	<i>Bcl3</i>	28.85
P0 <i>Dermo1-Ryk^{WT}</i>	<i>Ccl2</i>	30.03
P0 <i>Dermo1-Ryk^{CKO}</i>	<i>Ccl2</i>	30.78
P1 <i>Dermo1-Ryk^{WT}</i>	<i>Ccl2</i>	31.63
P1 <i>Dermo1-Ryk^{CKO}</i>	<i>Ccl2</i>	27.53
P2 <i>Dermo1-Ryk^{WT}</i>	<i>Ccl2</i>	31.28
P2 <i>Dermo1-Ryk^{CKO}</i>	<i>Ccl2</i>	27.67
P0 <i>Dermo1-Ryk^{WT}</i>	<i>Gapdh</i>	23.36
P0 <i>Dermo1-Ryk^{CKO}</i>	<i>Gapdh</i>	23.32
P1 <i>Dermo1-Ryk^{WT}</i>	<i>Gapdh</i>	25.29
P1 <i>Dermo1-Ryk^{CKO}</i>	<i>Gapdh</i>	24.35
P2 <i>Dermo1-Ryk^{WT}</i>	<i>Gapdh</i>	23.60
P2 <i>Dermo1-Ryk^{CKO}</i>	<i>Gapdh</i>	23.01

Fig. 3C

Sample Name	Gene Name	Ct mean
P0 <i>Dermo1-Ryk^{WT}</i>	<i>Casp4</i>	30.78
P0 <i>Dermo1-Ryk^{CKO}</i>	<i>Casp4</i>	30.43
P1 <i>Dermo1-Ryk^{WT}</i>	<i>Casp4</i>	31.40
P1 <i>Dermo1-Ryk^{CKO}</i>	<i>Casp4</i>	28.93
P2 <i>Dermo1-Ryk^{WT}</i>	<i>Casp4</i>	31.15
P2 <i>Dermo1-Ryk^{CKO}</i>	<i>Casp4</i>	28.36
P0 <i>Dermo1-Ryk^{WT}</i>	<i>Fas</i>	27.61
P0 <i>Dermo1-Ryk^{CKO}</i>	<i>Fas</i>	27.43
P1 <i>Dermo1-Ryk^{WT}</i>	<i>Fas</i>	28.86
P1 <i>Dermo1-Ryk^{CKO}</i>	<i>Fas</i>	27.31
P2 <i>Dermo1-Ryk^{WT}</i>	<i>Fas</i>	29.11
P2 <i>Dermo1-Ryk^{CKO}</i>	<i>Fas</i>	28.05
P0 <i>Dermo1-Ryk^{WT}</i>	<i>Gapdh</i>	22.53
P0 <i>Dermo1-Ryk^{CKO}</i>	<i>Gapdh</i>	23.08
P1 <i>Dermo1-Ryk^{WT}</i>	<i>Gapdh</i>	24.11
P1 <i>Dermo1-Ryk^{CKO}</i>	<i>Gapdh</i>	23.46
P2 <i>Dermo1-Ryk^{WT}</i>	<i>Gapdh</i>	24.26
P2 <i>Dermo1-Ryk^{CKO}</i>	<i>Gapdh</i>	24.61

Appendix, Fig. S3A

Sample Name	Gene Name	Ct mean
<i>Dermo1-Ryk^{WT}</i> -EpiC	<i>Ryk</i>	29.17
<i>Dermo1-Ryk^{CKO}</i> -EpiC	<i>Ryk</i>	27.56
<i>Dermo1-Ryk^{WT}</i> -EC	<i>Ryk</i>	29.83
<i>Dermo1-Ryk^{CKO}</i> -EC	<i>Ryk</i>	32.14
<i>Dermo1-Ryk^{WT}</i> -HC	<i>Ryk</i>	32.22
<i>Dermo1-Ryk^{CKO}</i> -HC	<i>Ryk</i>	32.35
<i>Dermo1-Ryk^{WT}</i> -MC	<i>Ryk</i>	26.10
<i>Dermo1-Ryk^{CKO}</i> -MC	<i>Ryk</i>	32.11
<i>Dermo1-Ryk^{WT}</i> -EpiC	<i>Gapdh</i>	26.03
<i>Dermo1-Ryk^{CKO}</i> -EpiC	<i>Gapdh</i>	24.55
<i>Dermo1-Ryk^{WT}</i> -EC	<i>Gapdh</i>	26.44
<i>Dermo1-Ryk^{CKO}</i> -EC	<i>Gapdh</i>	29.25
<i>Dermo1-Ryk^{WT}</i> -HC	<i>Gapdh</i>	22.96
<i>Dermo1-Ryk^{CKO}</i> -HC	<i>Gapdh</i>	22.63
<i>Dermo1-Ryk^{WT}</i> -MC	<i>Gapdh</i>	23.78
<i>Dermo1-Ryk^{CKO}</i> -MC	<i>Gapdh</i>	26.48

Appendix, Fig. S6B

Sample Name	Gene Name	Ct mean
P0 <i>Dermo1-Ryk^{WT}</i>	<i>Csf3</i>	32.24
P0 <i>Dermo1-Ryk^{CKO}</i>	<i>Csf3</i>	32.07
P1 <i>Dermo1-Ryk^{WT}</i>	<i>Csf3</i>	31.72
P1 <i>Dermo1-Ryk^{CKO}</i>	<i>Csf3</i>	30.06
P2 <i>Dermo1-Ryk^{WT}</i>	<i>Csf3</i>	31.45
P2 <i>Dermo1-Ryk^{CKO}</i>	<i>Csf3</i>	30.57
P0 <i>Dermo1-Ryk^{WT}</i>	<i>Cxcr2</i>	31.63
P0 <i>Dermo1-Ryk^{CKO}</i>	<i>Cxcr2</i>	31.03
P1 <i>Dermo1-Ryk^{WT}</i>	<i>Cxcr2</i>	32.97
P1 <i>Dermo1-Ryk^{CKO}</i>	<i>Cxcr2</i>	31.71
P2 <i>Dermo1-Ryk^{WT}</i>	<i>Cxcr2</i>	32.61
P2 <i>Dermo1-Ryk^{CKO}</i>	<i>Cxcr2</i>	31.89
P0 <i>Dermo1-Ryk^{WT}</i>	<i>Il1r9</i>	32.68
P0 <i>Dermo1-Ryk^{CKO}</i>	<i>Il1r9</i>	32.70
P1 <i>Dermo1-Ryk^{WT}</i>	<i>Il1r9</i>	34.59
P1 <i>Dermo1-Ryk^{CKO}</i>	<i>Il1r9</i>	30.62
P2 <i>Dermo1-Ryk^{WT}</i>	<i>Il1r9</i>	33.90
P2 <i>Dermo1-Ryk^{CKO}</i>	<i>Il1r9</i>	29.19
P0 <i>Dermo1-Ryk^{WT}</i>	<i>Il1r2</i>	31.15
P0 <i>Dermo1-Ryk^{CKO}</i>	<i>Il1r2</i>	29.95
P1 <i>Dermo1-Ryk^{WT}</i>	<i>Il1r2</i>	34.79
P1 <i>Dermo1-Ryk^{CKO}</i>	<i>Il1r2</i>	29.91
P2 <i>Dermo1-Ryk^{WT}</i>	<i>Il1r2</i>	35.92
P2 <i>Dermo1-Ryk^{CKO}</i>	<i>Il1r2</i>	31.06
P0 <i>Dermo1-Ryk^{WT}</i>	<i>Serpina3f</i>	27.97
P0 <i>Dermo1-Ryk^{CKO}</i>	<i>Serpina3f</i>	27.32
P1 <i>Dermo1-Ryk^{WT}</i>	<i>Serpina3f</i>	30.33
P1 <i>Dermo1-Ryk^{CKO}</i>	<i>Serpina3f</i>	25.93
P2 <i>Dermo1-Ryk^{WT}</i>	<i>Serpina3f</i>	30.30
P2 <i>Dermo1-Ryk^{CKO}</i>	<i>Serpina3f</i>	25.98
P0 <i>Dermo1-Ryk^{WT}</i>	<i>Gapdh</i>	23.36
P0 <i>Dermo1-Ryk^{CKO}</i>	<i>Gapdh</i>	23.32
P1 <i>Dermo1-Ryk^{WT}</i>	<i>Gapdh</i>	25.29
P1 <i>Dermo1-Ryk^{CKO}</i>	<i>Gapdh</i>	24.35
P2 <i>Dermo1-Ryk^{WT}</i>	<i>Gapdh</i>	23.60
P2 <i>Dermo1-Ryk^{CKO}</i>	<i>Gapdh</i>	23.01

Appendix, Fig. S6C

Sample Name	Gene Name	Ct mean
P0 <i>Dermo1-Ryk^{WT}</i>	<i>Ddit4</i>	33.86
P0 <i>Dermo1-Ryk^{CKO}</i>	<i>Ddit4</i>	31.66
P1 <i>Dermo1-Ryk^{WT}</i>	<i>Ddit4</i>	37.00
P1 <i>Dermo1-Ryk^{CKO}</i>	<i>Ddit4</i>	33.97
P2 <i>Dermo1-Ryk^{WT}</i>	<i>Ddit4</i>	36.63
P2 <i>Dermo1-Ryk^{CKO}</i>	<i>Ddit4</i>	35.19
P0 <i>Dermo1-Ryk^{WT}</i>	<i>Gadd45g</i>	27.35
P0 <i>Dermo1-Ryk^{CKO}</i>	<i>Gadd45g</i>	26.95
P1 <i>Dermo1-Ryk^{WT}</i>	<i>Gadd45g</i>	29.60
P1 <i>Dermo1-Ryk^{CKO}</i>	<i>Gadd45g</i>	29.60
P2 <i>Dermo1-Ryk^{WT}</i>	<i>Gadd45g</i>	29.29
P2 <i>Dermo1-Ryk^{CKO}</i>	<i>Gadd45g</i>	28.14
P0 <i>Dermo1-Ryk^{WT}</i>	<i>Pim1</i>	30.06
P0 <i>Dermo1-Ryk^{CKO}</i>	<i>Pim1</i>	29.15
P1 <i>Dermo1-Ryk^{WT}</i>	<i>Pim1</i>	32.07
P1 <i>Dermo1-Ryk^{CKO}</i>	<i>Pim1</i>	29.07
P2 <i>Dermo1-Ryk^{WT}</i>	<i>Pim1</i>	31.34
P2 <i>Dermo1-Ryk^{CKO}</i>	<i>Pim1</i>	29.98
P0 <i>Dermo1-Ryk^{WT}</i>	<i>Gapdh</i>	23.42
P0 <i>Dermo1-Ryk^{CKO}</i>	<i>Gapdh</i>	23.44
P1 <i>Dermo1-Ryk^{WT}</i>	<i>Gapdh</i>	24.15
P1 <i>Dermo1-Ryk^{CKO}</i>	<i>Gapdh</i>	23.09
P2 <i>Dermo1-Ryk^{WT}</i>	<i>Gapdh</i>	24.00
P2 <i>Dermo1-Ryk^{CKO}</i>	<i>Gapdh</i>	23.36

Appendix, Fig. S7D

Sample Name	Gene Name	Ct mean
Non-transfected	<i>Ryk</i>	19.22
EGFP siRNA	<i>Ryk</i>	18.87
<i>Ryk</i> siRNA 10 nM	<i>Ryk</i>	18.90
<i>Ryk</i> siRNA 50 nM	<i>Ryk</i>	18.80
Non-transfected	<i>Gapdh</i>	26.66
EGFP siRNA	<i>Gapdh</i>	26.13
<i>Ryk</i> siRNA 10 nM	<i>Gapdh</i>	28.16
<i>Ryk</i> siRNA 50 nM	<i>Gapdh</i>	29.68

Appendix, Fig. S6D

Sample Name	Gene Name	Ct mean
<i>Dermo1-Ryk^{WT}</i> -EpiC	<i>Bcl3</i>	31.47
<i>Dermo1-Ryk^{CKO}</i> -EpiC	<i>Bcl3</i>	28.71
<i>Dermo1-Ryk^{WT}</i> -EC	<i>Bcl3</i>	29.19
<i>Dermo1-Ryk^{CKO}</i> -EC	<i>Bcl3</i>	31.03
<i>Dermo1-Ryk^{WT}</i> -HC	<i>Bcl3</i>	26.00
<i>Dermo1-Ryk^{CKO}</i> -HC	<i>Bcl3</i>	25.24
<i>Dermo1-Ryk^{WT}</i> -MC	<i>Bcl3</i>	28.18
<i>Dermo1-Ryk^{CKO}</i> -MC	<i>Bcl3</i>	28.06
<i>Dermo1-Ryk^{WT}</i> -EpiC	<i>Ccl2</i>	35.51
<i>Dermo1-Ryk^{CKO}</i> -EpiC	<i>Ccl2</i>	31.09
<i>Dermo1-Ryk^{WT}</i> -EC	<i>Ccl2</i>	32.45
<i>Dermo1-Ryk^{CKO}</i> -EC	<i>Ccl2</i>	31.95
<i>Dermo1-Ryk^{WT}</i> -HC	<i>Ccl2</i>	28.00
<i>Dermo1-Ryk^{CKO}</i> -HC	<i>Ccl2</i>	27.24
<i>Dermo1-Ryk^{WT}</i> -MC	<i>Ccl2</i>	29.02
<i>Dermo1-Ryk^{CKO}</i> -MC	<i>Ccl2</i>	26.38
<i>Dermo1-Ryk^{WT}</i> -EpiC	<i>Casp4</i>	35.55
<i>Dermo1-Ryk^{CKO}</i> -EpiC	<i>Casp4</i>	32.28
<i>Dermo1-Ryk^{WT}</i> -EC	<i>Casp4</i>	31.59
<i>Dermo1-Ryk^{CKO}</i> -EC	<i>Casp4</i>	32.42
<i>Dermo1-Ryk^{WT}</i> -HC	<i>Casp4</i>	28.55
<i>Dermo1-Ryk^{CKO}</i> -HC	<i>Casp4</i>	27.41
<i>Dermo1-Ryk^{WT}</i> -MC	<i>Casp4</i>	33.25
<i>Dermo1-Ryk^{CKO}</i> -MC	<i>Casp4</i>	30.64
<i>Dermo1-Ryk^{WT}</i> -EpiC	<i>Fas</i>	34.04
<i>Dermo1-Ryk^{CKO}</i> -EpiC	<i>Fas</i>	31.78
<i>Dermo1-Ryk^{WT}</i> -EC	<i>Fas</i>	28.91
<i>Dermo1-Ryk^{CKO}</i> -EC	<i>Fas</i>	31.77
<i>Dermo1-Ryk^{WT}</i> -HC	<i>Fas</i>	28.12
<i>Dermo1-Ryk^{CKO}</i> -HC	<i>Fas</i>	27.15
<i>Dermo1-Ryk^{WT}</i> -MC	<i>Fas</i>	28.90
<i>Dermo1-Ryk^{CKO}</i> -MC	<i>Fas</i>	29.38
<i>Dermo1-Ryk^{WT}</i> -EpiC	<i>Gapdh</i>	25.53
<i>Dermo1-Ryk^{CKO}</i> -EpiC	<i>Gapdh</i>	24.21
<i>Dermo1-Ryk^{WT}</i> -EC	<i>Gapdh</i>	26.01
<i>Dermo1-Ryk^{CKO}</i> -EC	<i>Gapdh</i>	28.53
<i>Dermo1-Ryk^{WT}</i> -HC	<i>Gapdh</i>	22.47
<i>Dermo1-Ryk^{CKO}</i> -HC	<i>Gapdh</i>	22.61
<i>Dermo1-Ryk^{WT}</i> -MC	<i>Gapdh</i>	23.78
<i>Dermo1-Ryk^{CKO}</i> -MC	<i>Gapdh</i>	26.34

Dataset S1. Raw data of RNAseq analysis of P0 *Dermo1-Ryk^{WT}* and *Dermo1-Ryk^{CKO}* lungs